MATHEMATICAL BIOSCIENCES
AND ENGINEERING
Volume **7**, Number **1**, January **2010**

doi:10.3934/mbe.2010.7.171

pp. **171–185**

MODELING THE INTERACTION OF CYTOTOXIC T LYMPHOCYTES AND INFLUENZA VIRUS INFECTED EPITHELIAL CELLS

Abdessamad Tridane

Applied Sciences and Mathematics Department
Arizona State University at the Polytechnic campus, Mesa, Arizona, 85212, USA

Yang Kuang

School of Mathematics and Statistical Sciences
Arizona State University, Tempe, Arizona 85287, USA

Dedicated to Horst R. Thieme on the Occasion of his 60th Birthday

Abstract. The aim of this work is to investigate the mechanisms involved in the clearance of viral infection of the influenza virus at the epithelium level by modeling and analyzing the interaction of the influenza virus specific cytotoxic T Lymphocytes (CTL cells) and the influenza virus infected epithelial cells. Since detailed and definite mechanisms that trigger CTL production and cell death are still debatable, we utilize two plausible mathematical models for the CTLs response to influenza infection (i) logistic growth and (ii) threshold growth. These models incorporate the simulating effect of the production of CTLs during the infection. The systematical analysis of these models show that the behaviors of the models are similar when CTL density is high and in which case both generate reasonable dynamics. However, both models failed to produce the desirable and natural clearance dynamic. Nevertheless, at lower CTL density, the threshold model shows the possibility of existence of a "lower" equilibrium. This sub-threshold equilibrium may represent dose-dependent immune response to low level infection.

1. **Introduction.** The influenza virus is one of the major causes of disease worldwide. By now there is extensive knowledge on influenza virus and immunity following infection, but the virus can still catch us unprepared. This occurred during the 20th century, namely in 1918, 1957 and 1968 [22] and more recently in 2009 (Swine-flu [8]). The 1918 pandemic had the highest mortality, causing approximately 40 million deaths worldwide, with an unprecedented number of deaths of young adults [17]. If a pandemic with similar mortality occurred today then the number of deaths could, in a worst-case scenario, exceed 350 million people [17].

Influenza is a viral infection in which virions infect the epithelial cells of the upper respiratory tract and major central airways. The airway epithelium consists of a single layer of cells (everywhere except in the trachea) which is made up of at least four major cell types, including Basal cells (progenitor cells), Ciliated cells, Goblet cells, and Clara cells. The infection is characterized by desquamation (shedding or

2000 *Mathematics Subject Classification.* Primary: 34K20, 92C50; Secondary: 92D25.

Key words and phrases. influenza virus, immune response, cytotoxic T lymphocytes, mathematical model.

The research of Y. Kuang is supported in part by DMS-0436341 and DMS/NIGMS-0342388.

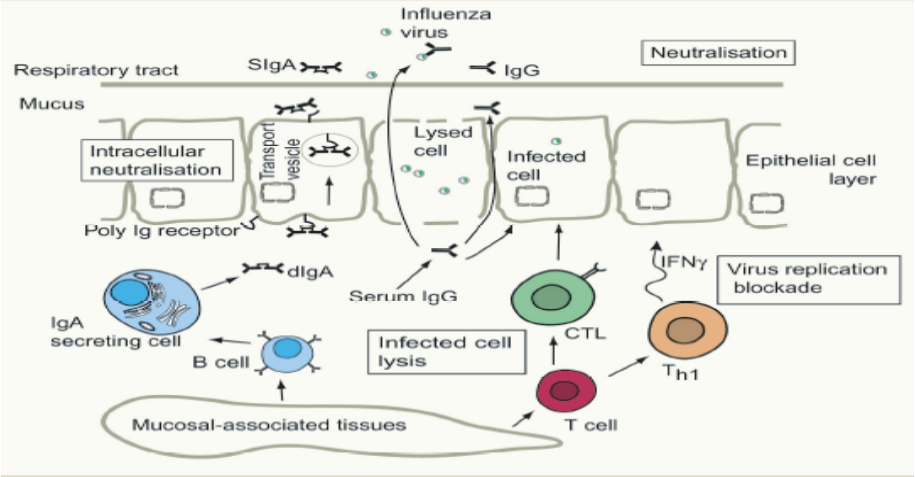

FIGURE 1. The mucosal immune system. There are four important mechanisms by which the mucosal immune system inhibits viral replication. 1) extracellular virus neutralization by antibody; 2) intracellular virus neutralization by transported IgA; 3) IFN-γ induce an antiviral state which inhibits viral replication in the cells of the mucosa; 4) lysis of infected cells by CTL cells. Adapted from [18].

peeling) of the epithelium of the nasal mucosa, the larynx, and the tracheobronchial tree (Fig. 1).

Influenza is transmitted via droplets expelled upon sneezing and coughing. The incubation period is usually 2-3 days before onset of illness, but it can be as long as 7 days. The patient is generally contagious during the febrile phase, but cases of viral spread have been observed prior to symptoms. The illness lasts approximately one week and is normally accompanied by high fever, headache, myalgia, sore throat, and rhinitis. Healthy people usually recover within one week without requiring medical intervention (Fig. 2).

The influenza virus, once inside an epithelial cell, subverts the metabolism of the cell to make more virus. Early in this process, these infected cells display fragments of the viral proteins in their surface class I histocompatibility (MHC) molecules. Certain $CD8^+$ cytotoxic T lymphocytes (CTLs) will be able to bind to these infected cells and destroy them before they can release newly synthesized viruses.

The dynamics of the immune system is highly complex and may produce effects which are difficult to interpret in terms of what is known about the individual components of the system. Differential equation models for cell populations with plausible assumptions on how these cells interact can provide some insight into such complex dynamics. Indeed, a variety of mathematical and computational models have been proposed in recent years in order to enhance our understanding of the within-host spread of diseases and the immune responses [7, 15, 3, 14, 1, 2, 16]. These existing models are either too simplistic and focused on the dynamic of the virus in mice [13], or without investigating in depth the CTL immune response in human [5], or too complex to handle mathematically [7].

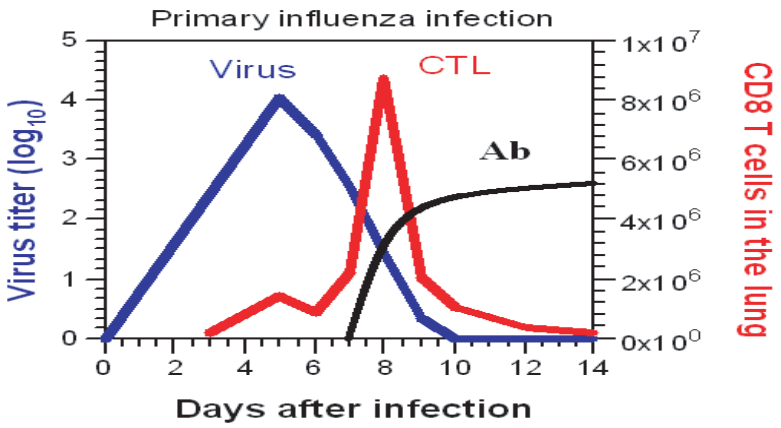

FIGURE 2. Immune response in the mouse model of influenza infection. Virus replicates exclusively in the epithelial cells lining the respiratory tract. Titers peak by day 5, and is cleared by day 8-10. $CD8^+$ CTLs appear at day 5 and antibody at day 7. Courtesy of [20].

The aim of this work is to identify some plausible mechanisms involved in the clearance of viral infection of the influenza virus at the epithelium level by modeling and analyzing the interaction of the influenza virus-specific $CD8^+$ CTLs and the epithelial cells. Since detailed and definite mechanisms that trigger CTL production and cell death are still controversial, we formulate alternative models of the CTL response to influenza infection for two plausible scenarios.

The first scenario is based on the logistic CTL growth. The qualitative behavior of this model is quite satisfactory as far as the time course of an actual infection is concerned. On the other hand, the saturation kinetics in the absence of the infectious agent may raise some doubts since a spontaneous increase of CTLs without an infectious agent cannot be explained. In the second scenario, we modify our first approach by introducing a threshold for CTL production.

We present a systematic analysis by investigating the effect of the CTL dependent basic reproduction number $R(T)$ on the infection clearance and persistence in the different dynamics of these models.

2. **The general model.** In the following, we will formulate and study the following plausible within-host influenza virus infection dynamics model

$$\begin{aligned}
\frac{dS}{dt} &= aS(1-S-I-J) - \beta SV \\
\frac{dI}{dt} &= \beta SV - \mu_1 I - bIT, \\
\frac{dJ}{dt} &= bIT - \mu_2 J, \\
\frac{dV}{dt} &= pI - \mu_3 V, \\
\frac{dT}{dt} &= \Phi(I,J,T) - bIT.
\end{aligned} \tag{1}$$

Where S is the density of uninfected epithelial cells, I is the density of infected epithelial cells, V is the density of virions, T is the density of CTLs and J is the density of pairs consisting of an infected cell and a CTL.

We assume that cell growth in the epithelium is mainly limited by space, which allows the density S to increase with rate a by dividing in order to fill up the gap created by the destroyed cells'. The virus infects host epithelial cells by binding to receptors on the cells surface via one major viral surface glycoprotein (HA) and replicates in the infected cells. We assume that the S cells become infected by virus at rate $\beta\frac{S}{N}V$, where β is the rate constant characterizing infection and $N =$ total epithelium space. For convenience, we assume the total epithelium space is 1. The newly synthesized viruses are released from the infected cells by the action of another major glycoprotein (NA) with an average rate of p per cell density. The infected cells are destroyed as a result of the cytopathic effect of the virions and as a result of the immune response. Specifically, the CTLs recognize (via the peptide-class I MHC complexes) and destroy infected cells with rate b. The natural apoptosis is considered at a rate of μ_1. Since our main goal is to study the immune response at the adaptive level, we will not consider the innate immune response. For simplicity, we will consider only the CTL immune response. The effects of adaptive immune responses on the virus are not explicitly described in this model; they are implicitly included in the virus clearance rate μ_3. We assume that the infected cells engaged by CTLs (J) are formed following the standard incidence ratio $b\frac{I}{N}T = bIT$ and cleared constant with rate μ_2.

The quantity $\Phi(I, J, T)$ is the net production rate for CTLs in the presence of free infected cells I and complexes J with CTLs. This function should be increasing in the variables I and J, and it should show a saturation kinetics with respect to T. Since we do not have detailed information on how the real system works, we assume that the saturation effect of the free T cells and the enhancing effect of existing infecting cells act additively, i.e., function Φ has a representation

$$\Phi(T, I + J) = \frac{1}{\tau}\phi(T) + \alpha(I + J). \tag{2}$$

Here $\tau > 0$ is the time constant of the CTL dynamics in the absence of any infection, and α is the rate at which the level of infection stimulates CTL production. Hence small τ describes a rapid CTL production, and large α describes quick reaction of the CTL production to an increased number of infected cells. We assume that function ϕ is selected from one of the following two scenarios.

Model I: Logistic CTL growth: $\phi(T) = T(1 - T/K)$.

In the absence of an infection, CTL density stays at level 0. But this level is unstable. If the infectious agent is introduced, then CTL density increases and approaches the stable level K.

Model II: Threshold CTL growth: $\phi(T) = T(T - \theta)(1 - T/K)/(K - \theta)$, with $0 < \theta < K$.

There is a threshold $\theta > 0$. The level $T = 0$ is stable. Once the presence of the infectious agent carries the CTL level above the threshold, then it will go towards the upper level K.

3. **Properties of solutions.** Model (1) describes the evolution of a cell population. Hence the cell densities should remain non-negative and bounded, in particular $S(t) + I(t) + J(t) \leq 1$, for $t > 0$, as long as the solution exists. These properties

imply global existence of the solutions. The functions ϕ in the three models are negative for large positive values of T.

Proposition 1. *All solutions in R^4_+ exist for all $t > 0$ and are attracted by the compact set*

$$M = \{(S, I, J, V, T) \in R^4_+ : S + I + J \le 1,\ V \le \frac{p}{\mu_3} + V(0),\quad T \le 1 + (1 + \alpha\tau)K\},$$

and the set M set is positively invariant.

Proof. A standard argument [19] shows that R^4_+ is positively invariant, i.e., non-negative initial data lead to non-negative solutions. By adding the first three equations of (1) we get $(d/dt)(S + I + J) \le aS(1 - (S + I + J))$ which implies that the S, I, J components of all non-negative solutions stay bounded, and for each solution $\limsup_{t\to+\infty}(S(t) + I(t) + J(t)) \le 1$ holds. Since $I \le 1$, then $\frac{dV(t)}{dt} \le p - \mu_3 V(t)$. Therefore, $V(t) \le \frac{p}{\mu_3} + V(0)e^{-\mu_3 t}$, which implies that $V(t) \le \frac{p}{\mu_3} + V(0)$. Further we have $\frac{dT(t)}{dt} \le 0$ for $T \ge 1 + (1 + \alpha\tau)K$. Hence T stays bounded and $\limsup_{t\to+\infty} T(t) \le 1 + (1 + \alpha\tau)K$. These inequalities hold as long as the solution exists. Hence, boundedness implies global existence. □

Key dynamic behaviors of epidemic models are often conveniently described in terms of the basic reproduction number R_0. The basic reproduction number is the mean number of secondary cases which is caused by a typical infection in a totally susceptible population in its lifetime in the absence of vaccination or other control policies. Although the concept of a basic reproduction number is widely used in epidemic modeling, its practical importance is limited since R_0 is difficult to determine in nature and often model dependent. Moreover, it is usually highly dependent on other equally difficult to determine parameters.

Here we apply the basic reproduction number concept to cell populations within the human host. Since our objective is to understand the interaction of the virus infection with the CTL response, we find the following generalized CTL level dependent basic reproduction number $R(T)$ of the virus useful in our model analysis effort.

Proposition 2. *The CTL density dependent basic reproduction number of the infected cells at the CTL density T is*

$$R(T) = \beta \frac{p}{\mu_1 + bT} \frac{1}{\mu_3}. \tag{3}$$

Proof. An infected cell, in its lifetime, can generate on average $v(T)$ amount of viruses where $v(T)$= mean life expectation of an infected cell at the CTL density $(1/(\mu_1 + bT))$ times its virus production rate (p). A virus has an average lifetime of $1/\mu_3$ and hence can produce on average $i(T)$ amount of infection where $i(T)=\beta/\mu_3$. Therefore, according to the definition, $R(T) = v(T)i(T)$. □

The Jacobian of the system (1) at an arbitrary point is given by

$$J = \begin{pmatrix} a(1 - 2S - I - J) - \beta V & -aS & -aS & -\beta S & 0 \\ \beta V & -\mu_1 - bT & 0 & \beta S & -bI \\ 0 & bT & -\mu_2 & 0 & bI \\ 0 & p & 0 & -\mu_3 & 0 \\ 0 & \alpha - bT & \alpha & 0 & -bI + \phi'(T)/\tau \end{pmatrix}.$$

As with most models of infection dynamics, we expect the stability of the infection free equilibrium $E_{T^*} = (1, 0, 0, 0, T^*)$ to play a key role in understanding the dynamics of model (1). Model I has two infection free equilibria $E_0 = (1, 0, 0, 0, 0)$ and $E_K = (1, 0, 0, 0, K)$ while Model II has three infection free equilibria $E_0 = (1, 0, 0, 0, 0)$, $E_K = (1, 0, 0, 0, K)$, and $E_\theta = (1, 0, 0, 0, \theta)$. At a disease free equilibrium the Jacobian simplifies to

$$J_0 = \begin{pmatrix} -a & -a & -a & -\beta & 0 \\ 0 & -\mu_1 - bT & 0 & \beta & 0 \\ 0 & bT & -\mu_2 & 0 & 0 \\ 0 & p & 0 & -\mu_3 & 0 \\ 0 & \alpha - bT & \alpha & 0 & \phi'(T)/\tau \end{pmatrix}. \tag{4}$$

The following proposition is straightforward.

Proposition 3. . *Let* $B = \mu_1 + \mu_3 + bT^*$,
$\lambda_- = -\frac{1}{2}(B + \sqrt{B^2 - 4\mu_3(\mu_1 + bT^*)(1 - R(T^*))})$,
and $\lambda_+ = \frac{1}{2}(-B + \sqrt{B^2 - 4\mu_3(\mu_1 + bT^*)(1 - R(T^*))})$. *At any disease free equilibrium* $E_{T^*} = (1, 0, 0, 0, T^*)$, *the Jacobian has* $-a, -\mu_2$, $\phi'(T^*)/\tau$, λ_- *and* λ_+ *as its eigenvalues.*

Observe that λ_+ is positive if and only if $R(T^*) > 1$.

In the absence of CTLs, i.e., when $T = 0$, the reproduction number is simply $R(0) = \frac{\beta p}{\mu_1 \mu_3}$. If $R(0) < 1$ then the disease dies out without the intervention of CTLs. As T increases, $R(T)$ decreases. This is to be expected since the larger the amount of CTLs present, the less the rate of infection. If $R(0) > 1$ then two scenarios might happen (1) large CTL level can eliminate the infection (2) CTLs cannot eliminate the infection. We will explore these scenarios in details in subsequent analysis.

Routine local stability analysis shows that in model I, the point $(1, 0, 0, 0, 0)$ is a saddle point. For $R(0) < 1$ it has an unstable manifold of dimension 1, and otherwise it has an unstable manifold of dimension 2. If $R(K) \leq 1$, then the point $(1, 0, 0, 0, K)$ is an attractor, otherwise it is a saddle point with an unstable manifold of dimension 1. Finally, consider model II. The point $(1, 0, 0, 0, 0)$ is an attractor for $R(0) \leq 1$ and a saddle point with unstable manifold of dimension 1 otherwise. The point $(1, 0, 0, 0, K)$ is an attractor for $R(K) \leq 1$ and otherwise a saddle point with unstable manifold of dimension 1. The point $(1, 0, 0, 0, \theta)$ is always a saddle point. If $R(\theta) < 1$ then its unstable manifold has dimension 1, otherwise it has dimension 2.

4. **Endemic equilibria.** In this section, we are interested in the conditions of existence and uniqueness of endemic equilibria. Recall an endemic equilibrium is a nonnegative equilibrium with positive value for I. At an equilibrium, the following equations hold:

$$\begin{aligned} aS(1 - S - I - J) - \beta SV &= 0 && (5) \\ \beta SV - \mu_1 I - bIT &= 0 && (6) \\ bIT - \mu_2 J &= 0 && (7) \\ pI - \mu_3 V &= 0 && (8) \\ \phi(T) + \tau\alpha(I + J) - \tau bIT &= 0. && (9) \end{aligned}$$

Although the limiting case $\tau = 0$, which corresponds to an infinitely fast CTL response, is not biologically meaningful, it provides mathematical insight. If $\tau = 0$ then the equation (9) says that at equilibrium, the value of T must be one of the zeros of the function ϕ.

Lemma 4.1. *Suppose (S, I, J, T) is an equilibrium with $I \neq 0$. Then the values of I and T satisfy the equations*

$$I = f(T), \quad I = \frac{1}{\tau} g(T) \tag{10}$$

where

$$f(T) = \frac{a(1 - 1/R(T))}{a(1 + \frac{b}{\mu_2} T) + \frac{\beta p}{\mu_3}}, \tag{11}$$

$$g(T) = \frac{\phi(T)}{bT(1 - \frac{\alpha}{\mu_2}) - \alpha}. \tag{12}$$

Proof. We look for equilibria with $I \neq 0$. Equations (7) and (8) give

$$J = \frac{b}{\mu_2} TI, \tag{13}$$

$$V = \frac{p}{\mu_3} I, \tag{14}$$

$$I + J = (1 + \frac{b}{\mu_2} T)I. \tag{15}$$

These equations determine J, V and $I + J$ in terms of I, assuming T is known.

Replacing V from (14) in equation (6) yields

$$S = \frac{\mu_3}{\beta p}(\mu_1 + bT) = \frac{1}{R(T)}. \tag{16}$$

By this equation S is uniquely determined by T, provided $I \neq 0$.

In equation (5) replace $I + J$ from (15) and S from (16). We obtain

$$a\left(1 - \frac{\mu_3(\mu_1 + bT)}{\beta p}\right) = \left(a(1 + \frac{b}{\mu_2} T) + \frac{\beta p}{\mu_3}\right) I. \tag{17}$$

This implies that $I = f(T)$ where $f(T)$ is given in (11). In equation (9) replace $I + J$ from (15). We obtain

$$\frac{1}{\tau}\phi(T) + \alpha(1 + \frac{b}{\mu_2} T)I - bTI = 0. \tag{18}$$

This implies that $I = \frac{1}{\tau} g(T)$ where $g(T)$ is given in (12).

The expressions (11) and (12) both represent the component I as a function of T. We equate these expressions and arrive at a scalar equation for T,

$$\tau f(T) = g(T). \tag{19}$$

Once $T > 0$ has been determined, then I, V, J, S can be uniquely determined from (11), (13), and (16), respectively. □

We have reduced the problem of finding the equilibria to the discussion of a scalar equation (19). Furthermore, we have two representations for the component I which determine the sign of I. Hence we have proved the following proposition.

Proposition 4. *For fixed $\tau > 0$, every solution $T \geq 0$ of the equation (19) yields an endemic equilibrium. If $\tau f(T) = g(T) > 0$ then $R(T) > 1$ and the solution is feasible (i.e., S, I, J, $V > 0$). If $\tau f(T) = g(T) < 0$ then $R(T) < 1$ and the solution is not feasible. If $\tau f(T) = g(T) = 0$ then $R(T) = 1$ and $\phi(T) = 0$.*

The proof of Lemma 4.1 provides further insight. At a feasible equilibrium we necessarily have $R(T) > 1$. Hence for the particular T the expressions $\phi(T)$ and $bT(1 - \alpha/\mu_2) - \alpha$ have the same sign. This fact allows us to locate the solutions in relation to the zeros of ϕ.

Now we represent equilibria by their projections in the $(T, \tau I)$-plane. There are always the uninfected equilibria on the axis $I = 0$. If we let the parameter τ run from 0 to infinity then the equilibria move on certain curves which can intersect in various ways to be described later. For the moment we consider only the case where such a curve passes through the T-axis, i.e., where I changes sign. At such a point $R(T) = 1$ and $\phi(T) = 0$ (and, since ϕ by assumption has only simple roots, the denominator of the function g is different from zero). Hence we know that at such points $R(T)$ changes from $R(T) < 1$ to $R(T) > 1$ and I from $I < 0$ to $I > 0$.

Suppose $R(0) > 1$, then define $\bar{T}$ as the infimum of all CTL levels at which the virus cannot persist. Hence define $\bar{T}$ by the condition $R(\bar{T}) = 1$ or explicitly by

$$\bar{T} = \frac{\mu_1}{b}(R(0) - 1). \tag{20}$$

The pole of the function g is located at

$$p = p(\alpha) = \frac{\alpha}{b(1 - \frac{\alpha}{\mu_2})}. \tag{21}$$

In the proofs it is sometimes easier to work with $p(\alpha)$ than with α itself. If α runs from 0 to μ_2 then $p(\alpha)$ runs from 0 to ∞ .

4.1. **Endemic equilibrium of model I.** Recall that for model I, we have $\phi(T) = T(K-T)/K$. Hence for model I, the equation (19) is equivalent to a cubic equation.

Proposition 5. *We consider the solutions of (19). Let $R(0) > 1$. There are two main cases.*

1. *$R(K) < 1$. There is no feasible endemic equilibrium.*
2. *$R(K) > 1$. There is a branch of infected stationary solutions parameterized by $\tau > 0$.*
   There are also two main cases.
   (a) *For α small, $0 < p(\alpha) < K$. If τ increases from 0 to ∞ then T decreases from K to $p(\alpha)$, and τI increases along this branch to ∞, but I increases from $f(K)$ to $f(p(\alpha))$.*
   (b) *For α large, $p(\alpha) > K$ or $p(\alpha) < 0$. If τ increases from 0 to ∞ then T increases from K to large values, and also τI increases to infinity while I decreases to zero.*

Proof. First observe that $R(K) < 1$ is equivalent to $\bar{T} < K$, and $R(K) > 1$ is equivalent with $\bar{T} > K$. Now the proof works by inspecting the intersections of the graphs of the functions g and τf, in particular the relative positions of zeros and poles (see Figure 3).

We consider first the case that $p(\alpha) \in (0, K)$. The function g is negative in $(0, p(\alpha))$ and goes to $-\infty$ for $T \to p(\alpha)$. For $T > p(\alpha)$ the function g decreases from large positive values, changes sign at $T = K$, and is negative for $T > K$.

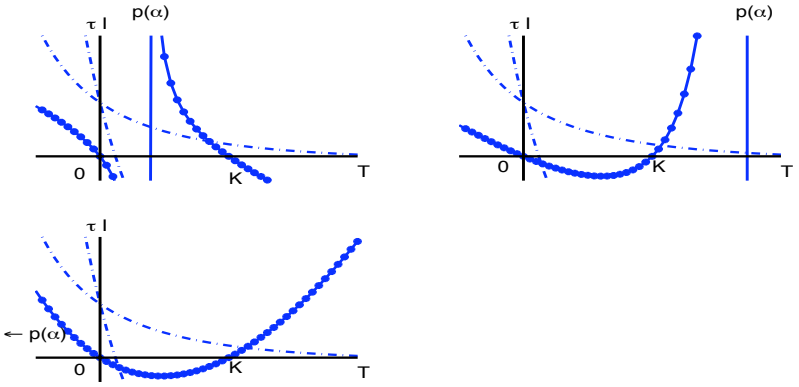

FIGURE 3. Schematic $(T, \tau I)$-plane for model I. The continuous line is the graph of the function g, the dashed lines are the graphs of the function τf, for $\bar{T}$ between 0 and K and for $\bar{T} > K$. The infected equilibrium exists if $\bar{T} > K$, and its position with respect to K depends on α.

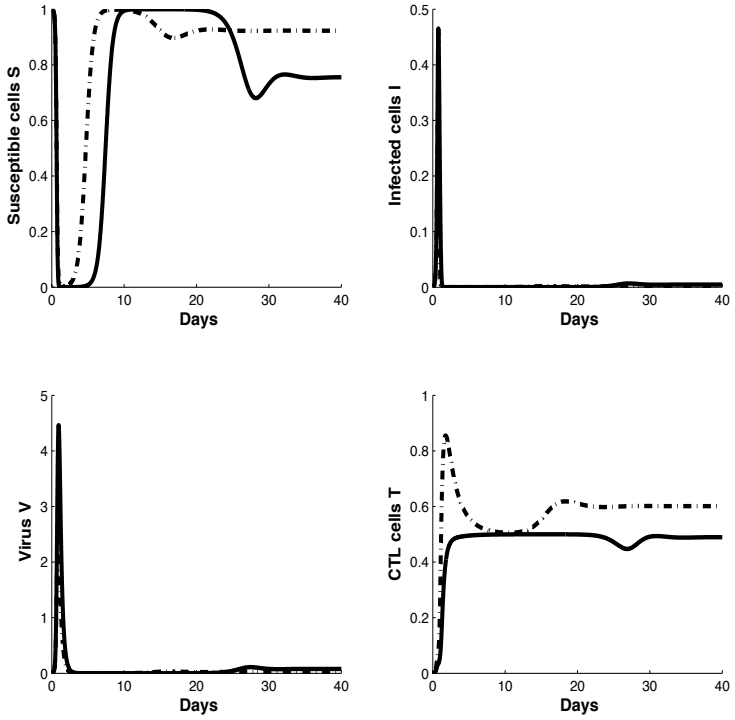

FIGURE 4. Model I, Time course of the variables S, I, J, V and T for $R(K) > 1$. For $p(\alpha) < K$ for $\alpha = 2.5$ (black line), $p(\alpha) < 0$ for $\alpha = 4.5$ (dashed line) . Here we have $\beta = 4, a = 2, b = 100, p = 50; \mu_3 = 3, \mu_1 = 1.4, \mu_2 = 2.7, K = 0.5$

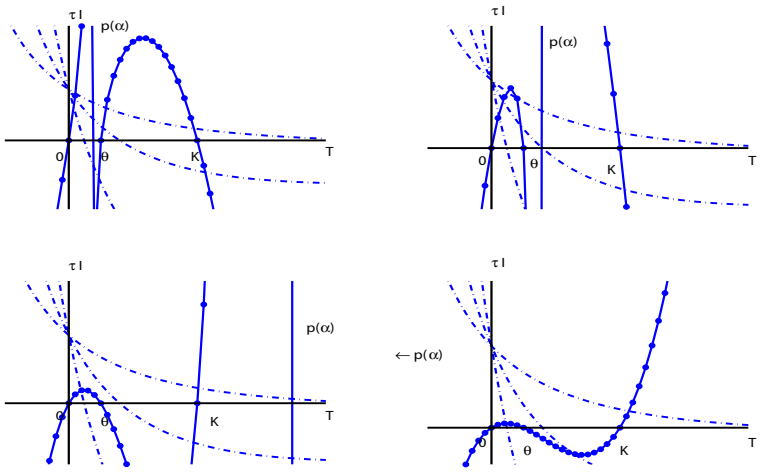

FIGURE 5. Schematic $(T, \tau I)$-plane for model II. Upper row: The pole is between 0 and θ or between θ and K. Lower row: The pole is above K or below 0. The dashed lines are the graphs of the function g, the dotted lines are the graphs of function τf for several positions of $\bar{T}$. An infected equilibrium exists if $\bar{T} > K$, and its position with respect to K depends on α. But there are also infected equilibria for small $\bar{T}$.

If $R(K) < 1$ then the function f is positive near $T = 0$ and changes sign to negative at $T = \bar{T} < K$. Hence there is an even number of intersections (no intersection if $\bar{T} < p(\alpha)$).

If $R(K) > 1$ then f changes sign at $\bar{T} > K$. There is an intersection. For small τ the intersection is near $T = K$. For increasing τ it moves towards smaller values of T but not below $p(\alpha)$. As τ increases and T decreases, τI increases towards infinity. If we compare the functions g/τ and f then we see that I increases towards $f(p(\alpha))$.

Consider now the case that $p(\alpha) > K$. The arguments are similar. The function g is negative for $T = 0$, then increases through 0 at $T = K$ towards the pole at $p(\alpha)$. Hence for $R(K) < 1$, i.e., $\bar{T} < K$, there is no intersection. For $R(K) > 1$ there is an intersection at some $T > K$. For small τ this intersection is near $T = K$. For increasing τ it moves towards the pole, τI increases to infinity while I converges to $f(p(\alpha))$. As for the case of $p(\alpha) < 0$, the arguments are verbally the same as in the preceding case.

In a projected phase plane for the variables T and I we have an uninfected state $(T, I) = (0, 0)$ which is a repeller. Then there is an uninfected state $(T, I) = (K, 0)$ which is either an attractor for $R(K) < 1$ or a saddle point for $R(K) > 1$. In the latter case there is an attracting infected equilibrium (see Fig. 4). □

According to this model, for large α the CTL cell eliminate the infection as expected(see Fig. 4). However, the saturation kinetics in the absence of the infectious agent may raise some doubts since a spontaneous increase of CTLs without an infectious agent cannot be explained immunologically. Therefore, we modify our model by introducing a threshold for CTL production.

4.2. **Endemic equilibria of model II.** Recall that for model II, we have $\phi(T) = T(T-\theta)(1-T/K)/(K-\theta)$. Again we assume that $R(0) > 1$.

Proposition 6. *We consider the solutions of (19). There are three main cases.*

1. $R(K) < R(\theta) < 1$. *For any α, there is a branch of infected equilibria with $T \in (0,\theta)$, parameterized by $\tau > 0$. For small τ the equilibrium is near $(0,0)$. As τ increases, T and τI increase while I stays bounded.*
2. $R(K) < 1 < R(\theta)$.
   (a) *α small, $p(\alpha) \in (0,\theta)$. There is a lower solution with $T \in (0,\theta)$ and an upper solution with $T \in (\theta, K)$.*
   (b) *α large, i.e., $p(\alpha) > \theta$ or $p(\alpha) < 0$. Then there is no solution (or an even number of solutions) with $T \in (\theta, K)$.*
3. $R(K) > 1$.
   (a) *α small, i.e., $p(\alpha) \in (0,\theta)$. There is always a solution with $T \in (0,\theta)$ and an even number of solutions with T in (θ, K).*
   (b) *α intermediate, $p(\alpha) \in (\theta, K)$. There is an even number of solutions in $(0,\theta)$ and a solution with T $(p(\alpha), K)$. Along this upper solution branch T is a decreasing function of τ.*
   (c) *α large, i.e., $p(\alpha) > K$ or $p(\alpha) < 0$. Then there is an even number of solutions with T in $(0,\theta)$ and a solution with $T > K$. Along this upper solution branch T in an increasing function of τ.*

Proof. For small τ there are three solution branches which start at the three zeros of ϕ, i.e., near $T = 0, \theta, K$.

First, consider the case where $0 < p(\alpha) < \theta$. The function g is positive between 0 and the pole at $p(\alpha)$, then negative between the pole and the zero θ, then again positive between the zeros θ and K. If τ is increased then along the first branch with $0 < T < \theta$ the quantity τI goes to infinity while the two other branches with $\theta < T < K$ eventually coalesce and disappear.

If $R(K) < R(\theta) < 1$ there is only one intersection that approaches to $(0,0)$ for τ small. For $R(K) < 1 < R(\theta)$ there are two intersections: one in $(0, p(\alpha))$ and the other in (θ, K) and finally for $R(K) > 1$ there is one intersection and possible two more τ large.

Consider now the case that $\theta < p(\alpha) < K$ (Fig. 5, top right panel). The function g is positive in $(0,\theta)$, negative between θ and the pole, then again positive between the pole and K, finally negative for $T > K$. If τ is increased then the first two branches coalesce and disappear while the third branch, with $T \in (p(\alpha), K)$ persists.

If $R(K) < R(\theta) < 1$ there is only one intersection that approaches $(0,0)$ for τ small. For $R(K) < 1 < R(\theta)$ there is no solution or even number of solutions (possible four if $\theta < p(\alpha) < \bar{T}$) . For $R(K) > 1$ there are one to three intersections depending on τ.

Finally, we consider cases that $K < p(\alpha)$ or $p(\alpha) < 0$ (Fig. 5, lower panels). The function g is positive in $(0,\theta)$, negative in (θ, K), and goes to infinity if T exceeds the value K (for $T \to p(\alpha)$ in the first case and for $T \to \infty$ in the second case). For small τ all three branches exist, for increasing τ the first two branches merge and disappear while the third branch persists with $T > K$.

If $R(K) < R(\theta) < 1$ there is only one intersection that approaches $(0,0)$ for τ small. For $R(K) < 1 < R(\theta)$ there is no solution or even number of solutions, and finally for $R(K) > 1$ there is one to three intersections depending on τ. □

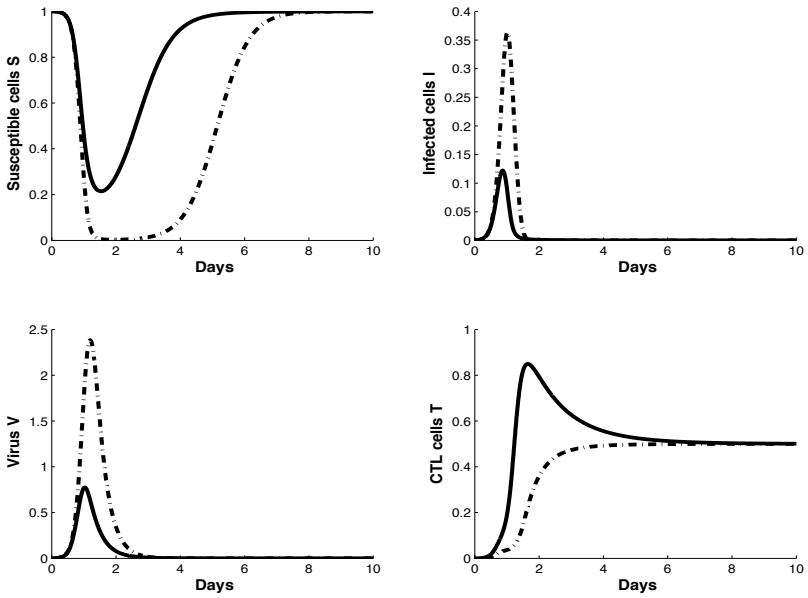

FIGURE 6. Model II, case (2) for $R(K) < 1 < R(\theta)$ and $p(\alpha) > \theta$ or $p(\alpha) < 0$ (solid line) and $p(\alpha) < \theta$ (dashed line). $\theta = 0.1, \beta = 4, \alpha = 6.5$ (2.5), $a = 2, b = 100, p = 30, \mu_3 = 3, \mu_1 = 1.4, \mu_2 = 2.7, K = 0.5$ For $\alpha = 6.5$ induce CTLs level to go up and return back to $K = 0.5$ after clearing the infection, and CTLs go to the hemostasis.

The (T, I) projected phase plane gives some insight into the (expected) qualitative behavior. We expect up to six stationary points.

There are three uninfected equilibria of the form $(0, 0)$, $(\theta, 0)$ and $(K, 0)$ and three infected equilibria of the general form (T_0, I_0), (T_θ, I_θ) and (T_K, I_K) which are located on the three branches of infected solutions. We know that the points $(0, 0)$ and $(K, 0)$ are stable with respect to T, and $(\theta, 0)$ is unstable. This stability pattern is inherited by the infected points for small τ. The point $(0, 0)$ is a saddle point, the point $(\theta, 0)$ is a repeller, and $(K, 0)$ is a saddle point again.

The point (T_0, I_0) and (T_K, I_K) are attractors separated by a basin boundary which contains (T_θ, I_θ) which is a saddle point. One of these attractors might disappear as τ increases depending on α.

In fact, consider in particular the case where $R(K) > 1$ and τ is not very close to zero. We follow the changes when α runs from small to large values. For small α there is the lower attractor with a low CTL level (below θ) and a rather high I. The two upper equilibria may not exist as τ becomes larger. If α is increased then the two lower equilibria need not exist for large τ but the upper equilibrium does exist, for medium α with $\theta < T < K$ and for large α with $T > K$.

Also, note that in the case where $R(K) < 1 < R(\theta)$ we have one only attractor which the lower equilibria for any value of τ.

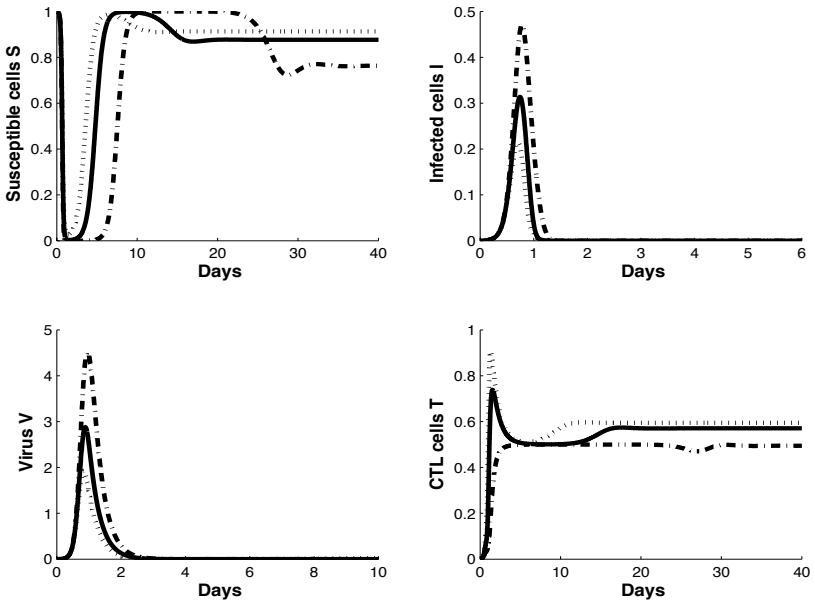

FIGURE 7. Model II, case (3) for $R(K) > 1$ and $\theta < p(\alpha) < K$ (dashed line), $0 < p(\alpha) < \theta$ (dots line) and finally $p(\alpha) < 0$ (solid line). Here using the following parameters $\theta = 0.1, \beta = 4, \alpha = 2.5, (6.5 \text{ and } 4.5 \text{ resp})\ a = 2, b = 100, p = 50, \mu_3 = 3, \mu_1 = 1.4, \mu_2 = 2.7, K = 0.5$.

So, as α increases and passes certain thresholds (most easily described in terms of $p(\alpha)$), the equilibrium CTL level increases, and we expect that the equilibrium I-level decreases.

5. **Discussion.** The underlying mechanisms of the adaptive cellular immune response in protecting the respiratory tract are yet to be fully studied [21]. To identify and better understand these mechanisms, we formulated and investigated some simplistic models of viral clearance of the influenza virus at the epithelium level. Specifically, we modeled and analyzed the interaction of the influenza virus-specific cytotoxic T Lymphocytes (CTL) and the infected epithelial cells. We introduced two different scenarios of CTL response. These models have some basic common features. There is an equilibrium CTL density K which can be reached once the immune response is triggered. The interaction of the infected cells with the CTLs is governed by a function $R(T)$ which is the reproduction number of the infection in the presence of a CTL response. The essential threshold condition is formulated in terms of $R(T)$. If $R(K) < 1$ then the CTL response can eliminate the infection. If $R(K) > 1$ then the CTL response cannot eliminate the infection.

In the first model we assume that there are no specific CTLs without an antigen. Once the CTL response is triggered, the CTLs interact with infected cells. It turns out that for α large the dynamic of CTL cell is similar qualitatively to the one describe in Fig 1, with decrease of CTL-cell, after clearing the infection, to level could be interpreted as level of CTL memory cells.

The second model is more speculative from the point of view of immune biology. Immunologists are convinced that there is no minimal dose with respect to viral or bacterial infections: in principle a single bacterium or virus can trigger an immune response. This fact does not contradict the possibility that infections from very small doses are very rare. One may expect a sigmoid dependence of the infection probability on the dose which may mimic a threshold. Again, the behavior near the CTL density K is similar to the previous the model (Fig 6, 7). The behavior at lower CTL levels is different, though. Depending on α, there may be subthreshold equilibria with a low CTL level even if $R(K) < 1$, or in addition to the standard "upper" equilibrium if $R(K) > 1$. The existence of these "lower" equilibria is a direct consequence of the threshold assumption. As mentioned above, we have replaced a dose-dependent probability by a threshold. In this view, the sub-threshold equilibria represent the assumed rare infections by small doses.

Our modeling approach shows that under familiar and plausible assumptions, models generate the standard threshold behavior of virus infection within a host population. If the basic reproduction number ($R(K)$) exceeds 1, then the infection persists. It is also true that if $R(K) < 1$ then in many situations the infection will be eliminated. Clearly, all these simplistic and plausible within-host influenza virus infection models fail to generate the biologically meaningful and desirable virus clearance outcome. Therefore, continued effort in searching for appropriate models that producing virus clearance following an infection episode is warranted. This is not only true for influenza virus infection, it is true for other virus infection as well ([6], [9], [10], [12]).

Acknowledgments. The authors would like to thank Professor Karl P. Hadeler for many substantial comments and suggestions. Also we thank the anonymous reviewer for her/his comments and suggestions

REFERENCES

[1] R. Antia and J. C. Koella, *A model of non-specific immunity*, Journal of Theoretical Biology, **168** (1994), 141–150.

[2] R. Antia, J. C. Koella and V. Perrot, *Models of the within-host dynamics of persistent mycobacterial infections*, Proceedings Royal Society of London: Biological Sciences, **263** (1996), 257–263.

[3] A. L. Asachenkov, G. I. Marchuk, R. R. Mohler and S. M. Zuev, *Immunology and disease control: A systems approach*, IEEE Trans on Biomedical Engineering, **41** (1994), 943–953.

[4] C. Beauchemin, J. Samuel and J. Tuszynski, *A simple cellular automaton model for influenza A viral infections*, Journal of Theoretical Biology, **232** (2005), 223–234.

[5] P. Baccam, C. Beauchemin, C. A. Macken, F. G. Hayden and A. S. Perelson, *Kinetics of influenza A virus infection in humans*, Journal of Virology, **80** (2006), 7590–7599.

[6] E. Beretta and Y. Kuang, *Modeling and analysis of a marine bacteriophage infection*, Math. Biosc., **149** (1998), 57–76.

[7] G. A. Bocharov and A. A. Romanyukha, *Mathematical model of aniviral immune response III. Influenza A virus infection*, Journal of Theoretical Biology, **167** (1994), 323–360.

[8] CDC, *Outbreak of swine-origin influenza A (H1N1) virus infection- Mexico*, March-April, 2009.

[9] S. Eikenberry, S. Hews, J. D. Nagy and Y. Kuang, *The dynamics of a delay model of HBV infection with logistic hepatocyte growth*, Math. Biosc. and Eng., **6** (2009), 283–299.

[10] S. A., Gourley, Y. Kuang and J. D. Nagy, *Dynamics of a delay differential model of hepatitis B virus infection*, J. Biological Dynamics, **2** (2008), 140–153.

[11] J. M. Heffernan, R. J. Smith and L. M. Wahl, *Perspectives on the basic reproductive ratio*, J. R. Soc. Interface, **2** (2005), 281–293

[12] S. Hews, S. Eikenberry, J. D. Nagy and Y. Kuang, *Rich dynamics of a hepatitis B viral infection model with logistic hepatocyte growth*, Journal of Mathematical Biology, (2009), in press.
[13] E. W. Larson, J. W. Dominik, A. H. Rowberg and G. A. Higbee, *Influenza virus population dynamics in the respiratory tract of experimentally infected mice*, Infect. Immun., **13** (1976), 438–447.
[14] G. I. Marchuk, "Mathematical Modelling of Immune Response in Infectious Diseases," Kluwer Academic Publishers, The Netherlands, 1997.
[15] M. A. Nowak and R. M. May, "Virus Dynamics," Oxford University Press, Oxford, United Kingdom, 2000.
[16] A. S. Perelson, *Modelling viral and immune system dynamics*, Nature Reviews Immunology, **2** (2002), 28–36.
[17] A. H. Reid, J. K. Taubenberger and T. G. Fanning, *The 1918 Spanish influenza: Integrating history and biology*, Microbes Infections, **3** (2001), 81–87.
[18] S. Tamura and T. Kurata, *Defense mechnisms against influenza infection in the respiratory tract mucosa*, Jpn. J. Infect. Dis., **57** (2004), 236–247.
[19] H. R. Thieme, "Mathematics in Population Biology," Princeton University Press, Princeton, 2003.
[20] D. J. Topham, "Mechanisms of T Cell Mediated Heterosubtype Immune Protection Against Influenza Virus," DIMACS workshop on the epidemiology and evolution of influenza, January 25 - 27, 2006.
[21] D. L. Woodland and L. Scott, *Cell memory in lung airways*, Proceedings of the American Thoracic Society, **2** (2005), 126–131.
[22] WHO, *Influenza pandemic preparedness and response*, Executive Board rapport, (2005) EB115/44: Geneva.

Received July 18, 2009; Accepted November 2, 2009.

E-mail address: Tridane@asu.edu
E-mail address: Kuang@asu.edu